

On Evaluation of Fracture Toughness for Mode III Crack Deformation

Ken-ichi HASHIMOTO*

Abstract

The evaluation of the fracture toughness for the materials has been established as the standard testing method in JSME and ASTM and is actively in use now. The stress fields near crack tips can be divided into three basic types each associated with a local mode of crack deformation and each crack deformation mode is independent. The standard tests are conducted for mode I crack deformation. The evaluation of the fracture toughness for mode II crack deformation is conducted as the combined mode evaluation with mode I because the mode II crack deformation is in-plane deformation. However, because the fracture toughness evaluation for mode III crack deformation is out-plane shear crack deformation, even the selection of the testing methods is difficult. Furthermore as the analytical solutions of the mode III stress intensity factor for two dimensional problem are analyzed with the strong restriction, we must use with severe care. With these backgrounds, there are not many examples in the study for the evaluation of mode III crack deformation. In this study, the evaluation of the mode III fracture toughness is performed in using the acryl resin specimens. As a result, the considerably lower values are obtained in comparison with the fracture toughness of mode I and mode II crack deformation.

Key Words : mode III crack deformation, fracture toughness, out-plane shear, stress intensity factor, acryl resin specimen

1. Introduction

The stress fields near crack tips can be divided into three basic types each associated with a local mode of crack deformation. The opening mode, I, is associated with local displacement in which the crack surfaces move directly apart. The edge-sliding mode, II, is characterized by displacement in which the crack surfaces slide over one another perpendicular to the leading edge of the crack. The tearing mode, III, finds the crack surfaces sliding with respect to one another parallel to the leading edge. As for the fracture for three crack deformation mode, it is well known experimentally and analytically that the fracture for the mode I loading occur with the crack along pre-existing crack surfaces and one for the mode II loading generate with the wing crack^{1),2)}. The crack extension behavior for the mode III loading is somewhat complicated. If the analytical models are approximated by the two dimensional models, the crack initiation from the pre-existing crack occurs with the crack along the pre-existing crack³⁾. However, as far as the analytical models

are treated as the three dimensional models under the mode III loading, the stress fields near crack tips is very complex⁴⁾⁻⁸⁾ and some kinds of cracks are observed. The echelon crack^{4),5),8)}, the petal cracks^{5),6),9),10)} and shell-like cracks^{7),9),10)}, for example.

The many analyses of the stress intensity factors for two dimensional (hereinafter referred to as 2-D) problems had been given by the various methods^{11),12)}. In these 2-D solutions of stress intensity factors(SIF), the analytical solution used most frequently is the stress intensity factor for the testing model of the fracture toughness evaluation¹³⁾. As these analytical solutions in mode I loading models and mode II loading models are treated as the in-plane problems, it is considered that three dimensional solutions(hereinafter referred to as 3-D) are similar to 2-D solutions except the stress intensity factors for the crack tips near the free surface. However, it is predicted that the 2-D analytical solutions for mode III loading models may be different from the 3-D solutions because the analytical solutions obtained as the out-of plane shear mode problems

* Department of Civil Engineering and Architecture

are given with the strong restriction within in-plane.

In this study, after the difference of theory between plane problem and three dimensional problem for the stress field near mode III crack tip is made clear, the evaluation of the fracture toughness for mode III crack deformation is conducted using the 2-D analytical solution. The material used in this experiment is the acryl resin which it has the stable material property and has been used widely in many experiments.

2. Theoretical background

The 2-D plane problem of a pure out- plane shear is described by next formulas.

$$u=0, \quad v=0, \quad w=w(x, y) \tag{1}$$

where $u, v,$ and w are the displacements of $x, y,$ and z -direction, respectively. The relationship between displacement and strain and Hooke's law are

$$\gamma_{xz} = \frac{\partial w}{\partial x} = \frac{\tau_{xz}}{G}, \quad \gamma_{yz} = \frac{\partial w}{\partial y} = \frac{\tau_{yz}}{G}, \tag{2}$$

where G is the modulus of elasticity in shear. All the stress components of $\sigma_x, \sigma_y, \sigma_z,$ and τ_{xy} are zero and the equation equilibrium for forces is

$$\frac{\partial \tau_{xz}}{\partial x} + \frac{\partial \tau_{yz}}{\partial y} = 0. \tag{3}$$

Next, the stress condition near crack tip for mode III crack deformation is three dimensionally considered. Simplifying the model which crack is subjected to the compressive loading, we can consider the model that the rectangle crack of ABCD with the slope of the angle γ exists in a parallelepiped as shown Fig.1. Here, the crack tips of AD and BC are dominated by the crack deformation mode of mode II and the crack tips of AB and DC are dominated by the crack deformation mode of mode III. The stress condition near the crack tip AB is investigated by using the model which the y -axis is taken in the extension line of BA, the x -axis is taken in the direction perpendicular to the surface ABCD, and the z -axis is taken in the extension line of DA as

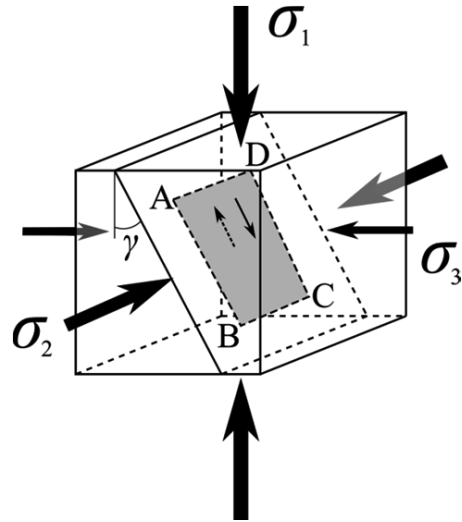


Fig.1 Crack under compressive loading

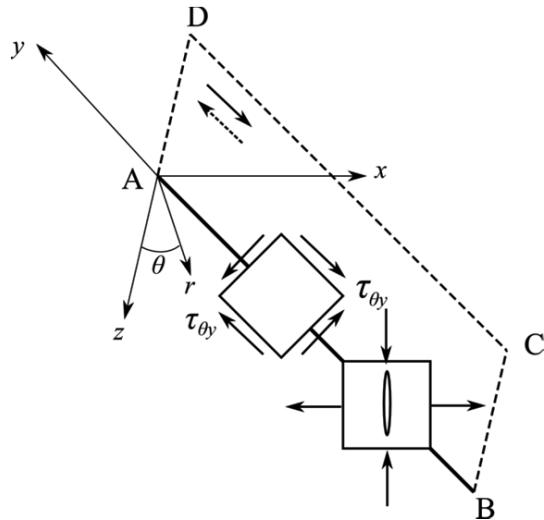


Fig.2 Echelon crack initiated in mode III crack

shown Fig.2. To generalized this discussion, the polar coordinate(r, θ) is considered to the x -axis from the z -axis. If we assume that $\theta = 0$, we obtained that $\tau_{\theta y} = \tau_{xy} = K_{III} / \sqrt{2\pi r}$, and $\tau_{yr} = \tau_{yz} = 0$. This stress condition is the pure shear stress condition due to $\tau_{\theta y}$. Therefore, very large tensile stress with the direction inclined $\pi/4$ clockwise and counterclockwise from the side AB occur near the crack tip AB as shown in the figure. This tensile stress induces the opening crack inclined $\pi/4$ clockwise from the side AB. When its crack surface is observed with the constant distance as shown in

Fig.3, those multiple cracks is called the echelon crack arrays. Based on these consideration results, the crack along the initial crack and the crack kinked from the initial crack are not generated, the crack intersected the initial crack tip line is generated at the one point of crack tip. However, the crack and a slip fault considered the pure shear fracture have been observed in many rock experiments and the surface of the earth.

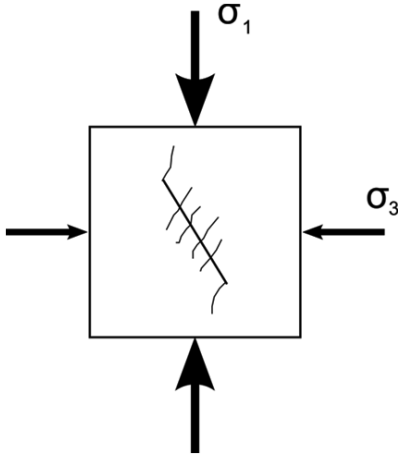


Fig.3 Wing crack and echelon cracks

In these discussion, the crack generation in 3-D elastic body with mode III loading can not be explained by 2-D theory.

3. Experiment

3.1 Summary of experiment

Single edge cracked strip subjected to concentrated shear forces on crack surface is applied to the experimental model. Its summary is shown in Fig.4 (a). The exact solution of SIF for this model is shown as follows¹⁴⁾.

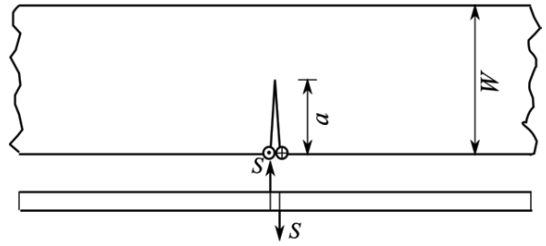
$$K_{III} = F_{III}(\alpha) \frac{2S}{\sqrt{\pi a}}, \quad \alpha = \frac{a}{W} \quad (4)$$

$$F_{III}(\alpha) = \sqrt{\frac{\pi a}{\sin \pi \alpha}}$$

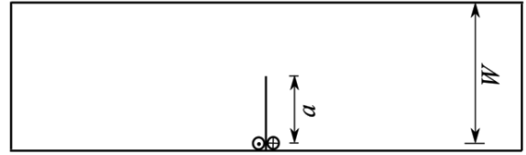
where S is the concentrated shear forces(See Fig.4 (a)).

2.2 Specimen

The acryl resin plate was used as the experimental specimen in this study. Chemical



(a) Summary of experimental model



(b) Experimental specimen

Fig.4 Experiment model and specimen

name is Methacrylic resin sheet and the trade name is SHINKOLITE™ which has been manufactured by Mitsubishi Rayon Co., Ltd. The important material properties are shown in Table 1. The fracture toughness values of mode I and mode II had

Table 1 Important material properties

Physical properties	JIS	Average value
Specific gravity	JIS K7112	1.19g/cm ³
Tensile strength	JIS K7113	75MPa
Flexural strength	JIS K7203	120MPa
Compressive strength	JIS K7181	120MPa
Modules of elasticity	JIS K7113	3.2 × 10 ³ MPa
Coefficient of thermal expansion	JIS K7197	7 × 10 ⁻⁵ C ⁻¹

been obtained in a range of 0.99~1.96MPa√m and 1.41~2.28 MPa√m, respectively^{15),16)}.

Specimens have the size with the width of 160mm, the length of 550mm, and the thickness of 2mm. Three specimens are prepared for the fracture experiment. The jigsaw was used in processing of the initial crack and crack length and crack width are about 80mm and 1mm, respectively. The crack tip is machined sharply using utility knife. Crack length(a) and specimen width(W) used in the evaluation of SIF are indicated in Table 2(See Fig.4(b)).

Table 2 Crack length and specimen width

Specimen number	Crack length a(mm)	Specimen width W(mm)
①	54.0	139.0
②	58.5	138.5
③	57.0	138.0

3.2 Experimental method

The desk universal material testing machine produced by TOKYO TESTING MACHINE INC. (Trade name; LITTLE SENSTAR, Stable capacity; 2000N) is employed in this experiment. Both edges of specimen are fixed by C type clamps in the frame connected by L type steel plate and straight steel plate. Two small C type clamps are fixed in the crack origin positions and these clamps and upper and lower jigs are connected by using the fine wire rope. With these procedures, mode III loading was carried out. Loading test is conducted with loading rate of 1mm/sec and datum of loading load and load point displacement are taken in the personal computer through data logger and GP-IB interface.

4. Experimental results

The relation between load and load point displacement for the specimen ② is shown in Fig.5. Load-displacement diagram has hardening behavior at an initial stage and presents the curve with convex slightly downward after that. Its shape can be regarded as the bi-linear line. The peak load

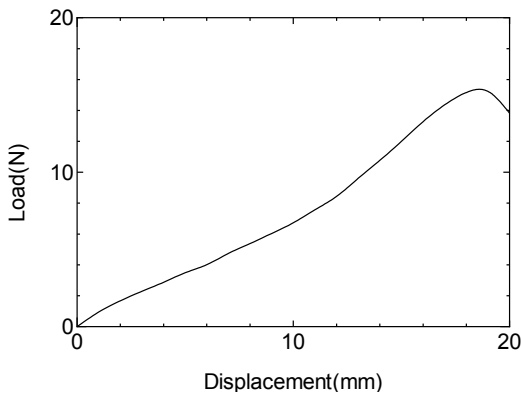
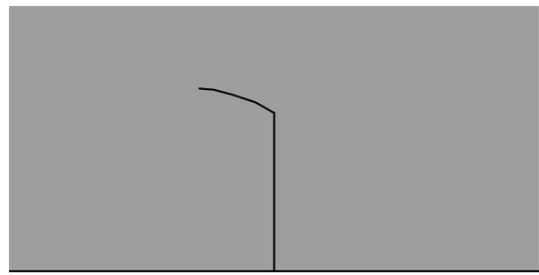


Fig.5 Load-load point displacement diagram

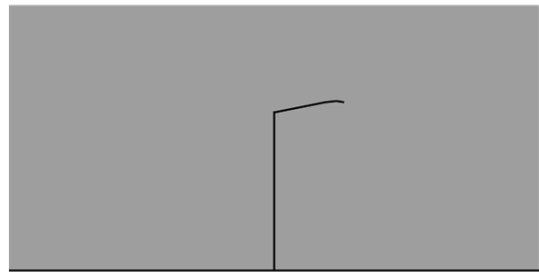
is recorded at the displacement with about 20mm.

Fracture crack growth behavior from an initial crack is shown in Fig.6. Fracture crack generates at an angle of $70^\circ \sim 75^\circ$ to the initial crack axis.

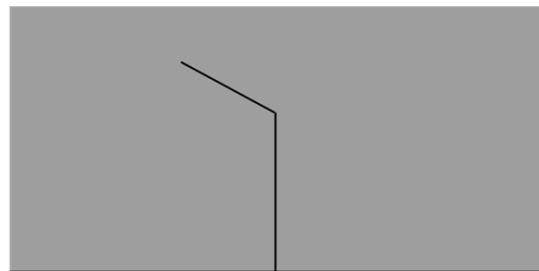
The evaluation results of mode III fracture toughness K_{IIIc} are shown in Table 2. The average value of the fracture toughness values obtained in this study is $0.041 \text{MPa}\sqrt{m}$. As it has been reported that the fracture toughness values of mode I and



(a) Crack extension state in specimen ①



(b) Crack extension state in specimen ②



(c) Crack extension state in specimen ③

Fig.6 Image diagram of fracture crack extension

mode II for acryl resin are in a range of $0.99 \sim 1.96 \text{MPa}\sqrt{m}$ and $1.41 \sim 2.28 \text{MPa}\sqrt{m}$, respectively as was stated previously, very small values are obtained in this evaluation as comparison with those fracture toughness values. Referring to rocks, K_{IIIc} of Westerly granite is $2.4 \text{MPa}\sqrt{m}$ as

Table 3 Evaluation results of mode III fracture toughness K_{IIIc}

Specimen number	Maximum load (N)	Displacement (mm)	$\alpha=a/W$	$F_{III}(\alpha)$	K_{IIIc} ($\text{N}/\text{mm}^{3/2}$)	K_{IIIc} ($\text{MPa}\cdot\text{m}^{1/2}$)
①	11.90	29.88	0.388	1.14	1.04	0.033
②	18.31	18.31	0.422	1.17	1.38	0.044
③	16.20	22.73	0.413	1.17	1.42	0.045

compared with $1.74 \text{ MPa}\sqrt{m}$ of K_{IC} and K_{IIIc} Solnhofen limestone is $1.3 \text{ MPa}\sqrt{m}$ as compared with $1.01 \text{ MPa}\sqrt{m}$ of K_{IC} ¹⁷⁾. Therefore, these rocks have some increase for K_{IIIc} as comparison with K_{IC} . However, there were the large difference between K_{IIIc} and K_{IC} of acryl resin.

5. Conclusion

In this study, after discussing the difference between 2-D theory and 3-D theory in mode III model, the evaluation of K_{IIIc} for the acryl resin specimens was conducted by using 2-D solution. As a result, the considerably smaller K_{IIIc} values were obtained as compared with K_{IC} of acryl resin and K_{IIIc} of rock. However, we can't have the result that 2-D solution of K_{III} can't be applied to the evaluation of the fracture toughness. Because the thickness of specimens used in the experiment is constant and thin. Therefore, the experiments using the specimens with various thicknesses and thick thickness will become necessary. Furthermore further study with 3-D numerical analysis and many experiments are necessary.

References

- 1) Erdogan, F., and Sih, G. C., "On the Crack Extension in Plates Under Plane Loading and Transverse Shear", ASME J. Basic Eng., 85(1963), pp.519-525.
- 2) Brace, W. F., and Bombolakis, E. G., "A Note on Brittle Crack Growth in Compression", J. Geophys. Res., 68(1963), pp.3709-3713.
- 3) Yatomi, C., Hashimoto, K., and Ishida, H., "Finite Element Analysis of the Energy Release Rate for a Kinked Crack Using the E-Integral", Lecture notes in Num. Appl. Anal., 13(1994), pp.61-74.
- 4) Cox, S. J. D., and Sholz, C. H., "On The formation and growth of faults: an experimental study", J. Struct. Geol.10(1988),pp.413-430.
- 5) Germanovich, L. N., Salganik, R. L., Dyskin, A. V., and Lee, K. K., "Mechanisms of Brittle Fracture of Rock with Pre-existing Cracks on Compression", Pure and Appl.Geophys.(PAGEOPH), 143(1994), pp.117-149.
- 6) Germanovich, L. N., Chater, B. J., Ingraffea, A. R., Dyskin, A. V., and Lee, K. K., "Mechanics of 3-D crack growth under compressive loads" Rock Meck. Auberin, Hassani & Mitri(eds),(Balkema, Rotterdam, 1996), pp.1151-1160.
- 7) Liang, Z. Z., Xing, H., Wang, S. Y. Williams, D. J., and Tang, C. A., "A three-dimensional numerical investigation of the fracture of rock specimens containing a pre-existing surface flaw", Comput. Geotech., 45(2012), pp.19-33.
- 8) Cox, S. J. D., and Sholz, C. H., "Rupture Initiation in Shear Fracture of Rock: An experimental study", J. Geophys. Res., 93(1988), pp.3307-3320.
- 9) Wong, R. H. C., Law, C. M., Chau, K. T., and Zhu, W., "Crack propagation from 3-D surface fractures in PMMA and marble specimens under uniaxial compression", Int. J. Rock Mech. Min. Sci.,41(2004), pp.360-366.
- 10) Liu, L. Q., Liu, P. X., Wong, H. C., Ma, S. P., and Gou, Y. S., "Experimental investigation of three- dimensional process from surface fault", Sci., China Ser. D-Earth. Sci.,51(2008), pp.1426-1435.
- 11) Rooke, D. P., and Cartwright, D. J., "Stress Intensity Factor", London Her Majesty's Stationery Office(1974).
- 12) Editor in chief Murakami, Y, "Stress Intensity Factor Handbook", Pergamon Press, Vol.1&2(1987), Vol.3(1992).
- 13) Srawley, J. E., "Wide range stress intensity factor expressions for ASTM E399 standard fracture toughness", Int. J. Fract. Mech. 12(1976), pp.475-476.
- 14) Sih G. C., "External cracks under longitudinal shear", J. Franklin Institute, 280(1965), pp.139-149.
- 15) Hashimoto, K., "Consideration on evaluation of fracture toughness evaluation of Mode II", Research Reports of The Tokuyama College of Technology, 31(2007), pp.7-12.
- 16) Hashimoto, K., "On consideration for fracture toughness and testing methods", Research Reports of The Tokuyama College of Technology, 27(2003), pp.31-35.
- 17) Scholz, C. H., "The mechanics and earthquakes and faulting", 2nd edition, Cambridge University Press, 1990, p.31.

(Received September 5, 2013)